

Development Status of Diffusion Code RAST-K 2.0 at UNIST

Minyong Park^a, Youqi Zheng^{a,b}, Jiwon Choe^a, Eunki Lee^c, Hocheol Shin^c, Peng Zhang^a, and Deokjung Lee^{a*},
^aSchool of Mechanical and Nuclear Engineering, UNIST, UNIST-gil 50, Ulsan, Republic of Korea
^bSchool of Nuclear Science and Technology, Xi'an Jiaotong University, Xi'an 710049, Shaanxi, China
^cKHNP-Central Research Institute, 1312-gil 70, Yuseong-gu, Daejeon 305-343, Republic of Korea
 *Corresponding author: deokjung@unist.ac.kr

1. Introduction

Diffusion code is one of the most important parts of a nuclear reactor design code package in two-step method. A lot of codes have been developed for the PWR reactor designs like SIMULATE-3, PARCS, MASTER, etc. [1, 2, 3]. In the past decades, these diffusion codes were well improved to fit to the requirement of new generation PWRs. In South Korea, a diffusion code RAST-K was developed by KHNP over 10 years ago [4]. A new version of RAST-K 2.0 is under development at Ulsan National Institute of Science and Technology (UNIST) since 2014. New computational models have been implemented for better performance. The target of RAST-K 2.0 is to be used in the analysis of current and future PWRs in South Korea design.

RAST-K 2.0 can be used to perform both steady-state and transient calculations. The non-linear scheme was used based on the 2-group CMFD and a three-dimensional multi-group unified nodal method (UNM) [5]. To consider the history effects, the main heavy isotopes were tracked by micro-depletion module using CRAM [6]. The simplified 1-D single channel thermal hydraulic solver from nTACER [7] is implemented. The θ method was adopted in the transient calculation. To get detailed pin-wise power and burnup distribution, Pin power reconstruction module was implemented. Also automatic control logic to calculate MTC, FTC, control rod worth was implemented. To perform multi-cycle analysis, restart and shuffling/rotation module has been implemented. To link between CASMO-4E [8] and RAST-K 2.0, CATORA (CASMO TO RAST-K 2.0) code was developed.

Unlike the other diffusion codes, RAST-K 2.0 depletion module uses CRAM and extended depletion chain for fission products. Most lattice codes give cumulative fission yield of Pm-149 without considering Pm-148 and Pm-149 capture reaction which will lead to the increase of Sm-149 number density. Therefore, Sm-149 number density can be calculated to be slightly lower in high burnup in the other diffusion codes.

In the verification, Shin-Kori Unit-1 cycle-01 OPR1000 PWR core from current nuclear power plants in South Korea were modelled. The parameters including critical boron concentration, radial and axial power distributions were compared with the references from the widely used CASMO-4E/SIMULATE-3 code system.

2. Cross-section Linkage

CATORA makes XS set table file for RAST-K 2.0 using the data from CAX files which is output file of CASMO-4E. The XS set table consists of branch and history calculation data, microscopic cross sections of specific nuclides, macroscopic cross sections of residual nuclides, fission yields of fission products, initial number densities of initial loaded nuclides, heterogeneous form functions, assembly discontinuity factors, surface neutron fluxes and currents, and kinetics parameters. Cross-section formulation is a function of control rod, burnup, boron concentration, fuel temperature, and moderator temperature. STORA (STREAM TO RAST-K) [9] is also under development to transfer the cross section data from STREAM to RAST-K 2.0.

3. Methods in Micro Depletion Module

2.1 Depletion Chain

To well consider the history effects in the PWR operation, the micro-depletion capability is developed in RAST-K 2.0. The nuclide number densities of 22 heavy isotopes and 12 fission products were tracked in the core calculation.

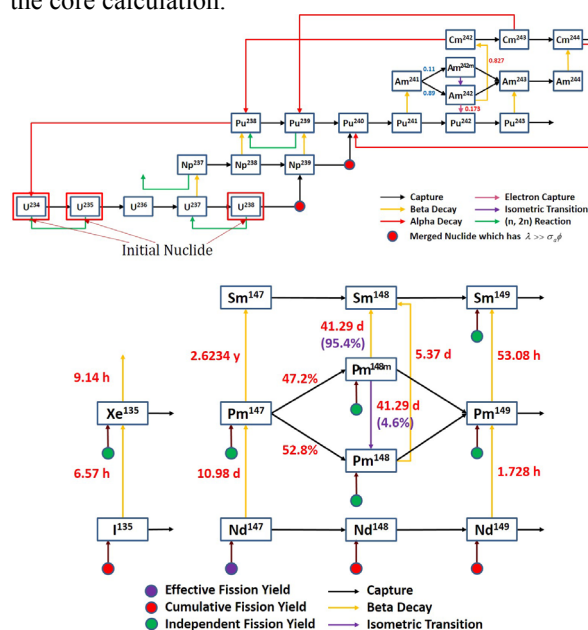


Fig. 1. Depletion chain of RAST-K 2.0.

2.2 Nuclide Data

Decay constant are used from the ENDF/B-VI.8. Table 1, 2 show the decay constants of heavy nuclides and fission products. Decay constants of nuclides which have half-life longer than 150 years are approximated to be zero.

Table 1. Decay constants of 12 heavy nuclides

No.	N_ID	Half Life					Decay Constant	Decay Type
		[m]	[h]	[d]	[y]	[sec]		
1	U-237			6.75		5.83200E+05	1.18852E-06	Beta-
2	Np-238			2.117		1.82909E+05	3.78958E-06	Beta-
3	Np-239			2.355		2.03472E+05	3.40660E-06	Beta-
4	Pu-238				87.76	2.76760E+09	2.50451E-10	Alpha
5	Pu-241				14.36	4.52857E+08	1.53061E-09	Beta-(99.99761%) Alpha(0.00239%)
6	Pu-243		4.956			1.78416E+04	3.88501E-05	Beta-
7	Am-242		16.02			5.76720E+04	1.20188E-05	Beta-(82.7%) EC(17.3%)
8	Am-242m				141.09	4.44941E+09	1.55784E-10	IT(99.55%) Alpha(0.45%)
9	Am-244		10.1			3.63600E+04	1.90635E-05	Beta-
10	Cm-242			162.9		1.40780E+07	4.92361E-08	Alpha
11	Cm-243			28.52		8.99407E+08	7.70672E-10	Alpha
12	Cm-244			18.11		5.71117E+08	1.21367E-09	Alpha

Table 2. Decay constants of 8 fission products

No.	N_ID	Half Life					Decay Constant	Decay Type
		[m]	[h]	[d]	[y]	[sec]		
1	I-135		6.57			2.36520E+04	2.93061E-05	Beta-
2	Xe-135		9.14			3.29040E+04	2.10657E-05	Beta-
3	Nd-147			10.98		9.48672E+05	7.30650E-07	Beta-
4	Nd-149		1.728			6.22080E+03	1.11424E-04	Beta-
5	Pm-147				2.6234	8.27315E+07	8.37827E-09	Beta-
6	Pm-148			5.37		4.63968E+05	1.49395E-06	Beta-
7	Pm-148m			41.29		3.56746E+06	1.94297E-07	Beta-
8	Pm-149		53.08			1.91088E+05	3.62737E-06	Beta-

CASMO-4E does not print (n, 2n) microscopic cross section of U-235, so it calculated approximately by Eq. (1).

$$\sigma_{(n,2n),g}^{U-235} = 0.71 \times \sigma_{(n,2n),g}^{U-238} \quad (1)$$

For improved accuracy of Sm-149 number density, RAST-K 2.0 solves neodymium chain. But CASMO-4E also does not print fission yield of Nd-147/148/149, so these values are calculated by Eq. (2) in CATORA. 'i' is fission nuclide index and 'j' is heavy nuclide index. Effective fission yield is 'cumulative fission yield + generation portion from other nuclide' and it is also calculated in CATORA. Eq. (3) shows the case of only i-1 nuclide's capture ('i' is mass number) and 'F' is total fission reaction rate. To calculate this, fission yield of 18 heavy nuclides are used from the ENDF/B-VI.8 as shown in Table. 3. Fission yields of heavy nuclides which do not exist in this table are assumed to be zero.

$$Y^i = \frac{\sum_{g=1}^2 \sum_{j=1}^{18} N_j \sigma_j^{f,g} \phi^g Y_j^{i,g}}{\sum_{j=1}^{18} N_j \langle \sigma_j^f | \phi \rangle} \quad (2)$$

$$Y_i^E = Y_i^C + \frac{a_{i-1} N_{i-1}}{F} \quad (3)$$

Table 3. Fission yields of 18 heavy nuclides (Fast/Thermal)

NO.	I_ID	Nd-147(F)	Nd-147(T)	Nd-148(F)	Nd-148(T)	Nd-149(F)	Nd-149(T)
1	U-234	2.01770E-02	2.01770E-02	1.43450E-02	1.43450E-02	1.03570E-02	1.03570E-02
2	U-235	2.13890E-02	2.24670E-02	1.68340E-02	1.67350E-02	1.03700E-02	1.08160E-02
3	U-236	2.29530E-02	2.29530E-02	1.72920E-02	1.72920E-02	1.33840E-02	1.33840E-02
4	U-237	2.61640E-02	2.61640E-02	1.85700E-02	1.85700E-02	1.44260E-02	1.44260E-02
5	U-238	2.59270E-02	2.59270E-02	2.11250E-02	2.11250E-02	1.62530E-02	1.62530E-02
6	Np-237	2.22780E-02	2.50000E-02	1.71940E-02	1.65850E-02	1.30240E-02	1.54720E-02
7	Np-238	2.39210E-02	2.39210E-02	1.77020E-02	1.77020E-02	1.75030E-02	1.75030E-02
8	Pu-238	2.23650E-02	2.23650E-02	1.75730E-02	1.75730E-02	1.59670E-02	1.59670E-02
9	Pu-239	1.99060E-02	2.00300E-02	1.66140E-02	1.64210E-02	1.24080E-02	1.21630E-02
10	Pu-240	2.20290E-02	2.12340E-02	1.77400E-02	1.77250E-02	1.33520E-02	1.39390E-02
11	Pu-241	2.22420E-02	2.28500E-02	1.95620E-02	1.93210E-02	1.45860E-02	1.47410E-02
12	Pu-242	2.37060E-02	2.38770E-02	2.00130E-02	1.99070E-02	1.57340E-02	1.59840E-02
13	Am-241	2.14930E-02	2.03240E-02	1.90250E-02	1.82920E-02	1.56980E-02	1.43230E-02
14	Am-242m	2.46680E-02	2.46880E-02	2.13350E-02	2.13350E-02	1.71940E-02	1.71940E-02
15	Am-243	2.33610E-02	2.33610E-02	1.86560E-02	1.86560E-02	1.5550E-02	1.5550E-02
16	Cm-242	2.17940E-02	2.17940E-02	1.80140E-02	1.80140E-02	1.46260E-02	1.46260E-02
17	Cm-243	2.68940E-02	2.09220E-02	2.38980E-02	2.35300E-02	1.98180E-02	1.98330E-02
18	Cm-244	2.88150E-02	2.88150E-02	2.48390E-02	2.48390E-02	2.08830E-02	2.08830E-02

2.3 Depletion Calculation Method

For the depletion calculation, the matrix form of Bateman equation was solved numerically except for I-135 and Xe-134 which were solved analytically:

$$\mathbf{A} = [a_{ij}]$$

$$a_{ii} = -(\lambda_i + \sum_{g=1}^G \sigma_{a,ig} \phi_g)$$

$$a_{ij} = \ell_{ji} \lambda_j + \gamma_{ji} \sum_{g=1}^G \sigma_{\gamma,jg} \phi_g \quad (4)$$

where

ℓ_{ji} = decay fraction (nuclide j to i)

λ_j = decay constant

ϕ_g = multi-group flux

γ_{ji} = production yield of nuclide i
by neutron reaction of nuclide j

$$\dot{\mathbf{N}} = \mathbf{A}\mathbf{N} + \mathbf{b}, \quad \mathbf{N} = e^{\mathbf{A}t} \mathbf{N}_0 + (e^{\mathbf{A}t} - \mathbf{I}) \mathbf{A}^{-1} \mathbf{b} \quad (5)$$

The CRAM method approximates this exponential matrix as:

$$e^{\mathbf{A}t} = \alpha_0 \mathbf{I} + 2 \operatorname{Re} \left[\sum_{i=1}^{k/2} \alpha_i (\mathbf{A}t - \theta_i \mathbf{I})^{-1} \right], \quad (6)$$

where k is CRAM approximation order and α_i, θ_i are partial fraction decomposition coefficients. In RAST-K 2.0, k is 16 and α_i, θ_i are shown in Table 4, 5.

Table 4. CRAM coefficients α_i

i	α_i	
	Real Part	Imaginary Part
0	2.12485371049523E-16	0
1	- 5.0901521865224915650E-7	- 2.4220017652852287970E-5
2	+ 2.1151742182466030907E-4	+ 4.3892969647380673918E-3
3	+ 1.1339775178483930527E+2	+ 1.0194721704215856450E+2
4	+ 1.5059585270023467528E+1	- 5.7514052776421819979E+0
5	- 6.4500878025539646595E+1	- 2.2459440762652096056E+2
6	- 1.4793007113557999718E+0	+ 1.7686588323782937906E+0
7	- 6.2518392463207918892E+1	- 1.1190391094283228480E+1
8	+ 4.1023136835410021273E-2	- 1.5743466173455468191E-1

Table 5. CRAM coefficients θ_i

i	θ_i	
	Real Part	Imaginary Part
1	- 1.0843917078696988026E+1	+ 1.9277446167181652284E+1
2	- 5.2649713434426468895E+0	+ 1.6220221473167927305E+1
3	+ 5.9481522689511774808E+0	+ 3.5874573620183222829E+0
4	+ 3.5091036084149180974E+0	+ 8.4361989858843750826E+0
5	+ 6.4161776990994341923E+0	+ 1.1941223933701386874E+0
6	+ 1.4193758971856659786E+0	+ 1.09253634844496722585E+1
7	+ 4.9931747377179963991E+0	+ 5.9968817136039422260E+0
8	- 1.4139284624888862114E+0	+ 1.3497725698892745389E+1

In case of heavy nuclide depletion chain, there is no vector \mathbf{b} . In case of fission product depletion chain, vector \mathbf{b} is fission yield term as in Eq. (7). This vector is needed to split fission product depletion chain from the total nuclide depletion chain. Since this method reduces the size of depletion chain, it can reduce the matrix operation time.

$$b_i = Y_i F \quad (7)$$

4. Numerical Results

To verify the depletion solver, C-1 type fuel assembly with gadolinia is solved. In this assembly depletion calculation, the critical spectrum option of CASMO-4E is off and T/H conditions are fixed. Also thermal expansion effects are considered such as geometry expansion (radius of fuel, gap, clad and guide tube, fuel height) and density decrease of fuel. Thermal expansion correction has more than 100 pcm k-inf improvement in one assembly depletion calculation.

To compare Pm-149/Sm-149 chain using analytic solution with cumulative fission yield of Pm-149 without considering Pm-148 and Pm-149 capture reaction which will lead to increase the number density of Sm-149 and Nd/Pm/Sm extended chain, RAST-K 2.0 sets the number densities of other nuclides are same with CASMO-4E results to avoid error from the other nuclides. From Figs. 2 and 3, cumulative fission yield correction by addition of capture reaction portion shows very accurate results until 60 GWD/MTU.

To verify core depletion capability, Shin-Kori Unit-1 cycle-01 has been calculated. Fig. 4. shows the difference of critical boron concentration is smaller than ± 7 ppm. Figs. 5. and 6. show BOC and EOC radial and axial normalized power distributions. RAST-K 2.0 compares well with SIMULATE-3.

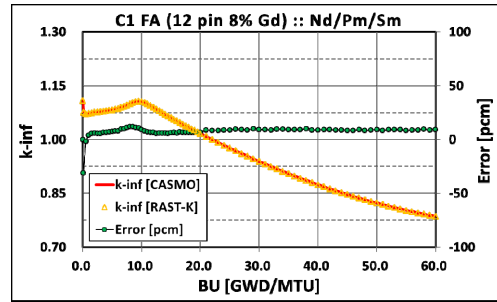


Fig. 2. k-inf of C1 fuel assembly [Pm-149/Sm-149 vs. Extended Nd/Pm/Sm].

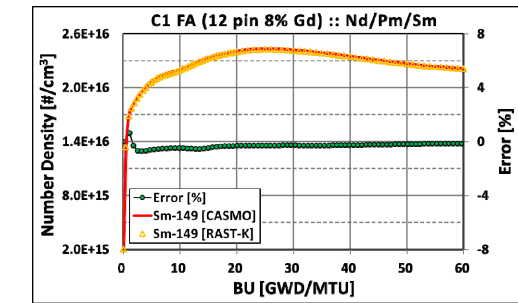
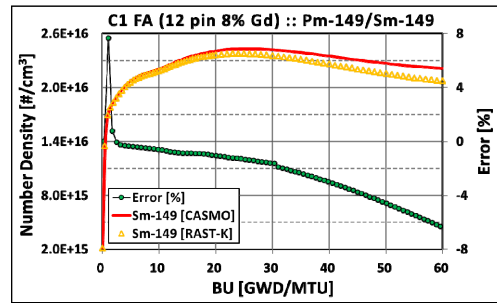


Fig. 3. Number density of Sm-149 of C1 fuel assembly [Pm-149/Sm-149 vs. Extended Nd/Pm/Sm].

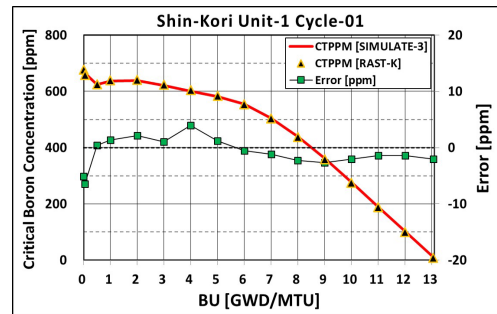
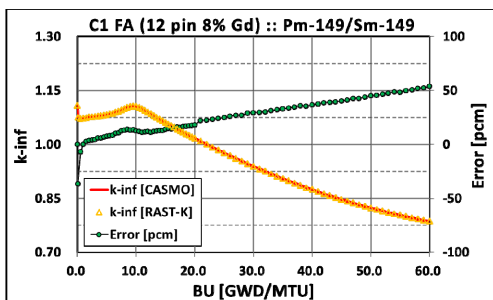


Fig. 4. Boron letdown curve for Shin-Kori Unit-1 cycle-01 [SIMULATE-3 vs. RAST-K 2.0]



5. Conclusions

This paper reports the status of RAST-K 2.0 code development at UNIST. The new code applies a new kernel based on the two-node UNM with CMFD, and θ method for kinetic calculation. Also, the micro-depletion calculation is used to consider the history effects. And other modules and functions also implemented such as pin power reconstruction, branch calculation, restart, multi-cycle, and 1-D single channel T/H solver. Especially RAST-K 2.0 has a unique micro-depletion module compared to the other diffusion codes, and its accuracy was verified with Shin-Kori Unit-1 cycle-01 and a fuel assembly problem.

Shin-Kori Unit-1 Cycle-01 (BOC, HFP, ARO)								
0.773	0.820	0.886	1.254	0.938	0.948	1.188	1.002	
0.786	0.833	0.899	1.260	0.946	0.952	1.184	0.983	
1.67	1.53	1.51	0.48	0.87	0.46	-0.38	-1.86	
0.820	0.841	1.222	0.947	1.273	0.933	1.166	0.850	
0.833	0.854	1.228	0.958	1.273	0.938	1.162	0.845	
1.53	1.58	0.51	1.14	0.03	0.53	-0.34	-0.54	
0.886	1.222	0.945	1.295	0.958	1.194	1.039	0.613	
0.899	1.228	0.957	1.297	0.965	1.191	1.034	0.610	
1.51	0.51	1.23	0.19	0.69	-0.23	-0.52	-0.51	
1.254	0.947	1.295	0.982	1.239	0.882	0.983		
1.260	0.958	1.297	0.989	1.238	0.884	0.963		
0.48	1.14	0.19	0.73	-0.08	0.21	-2.03		
0.938	1.273	0.958	1.239	1.167	0.995	0.595		
0.946	1.273	0.965	1.238	1.165	0.989	0.588		
0.87	0.03	0.69	-0.08	-0.14	-0.61	-1.13		
0.948	0.933	1.194	0.882	0.995	0.716			RMS 0.96
0.952	0.938	1.191	0.884	0.989	0.704			Min 0.03
0.46	0.53	-0.23	0.21	-0.61	-1.74			Max 2.03
1.188	1.166	1.039	0.983	0.595				
1.184	1.162	1.034	0.963	0.588				
-0.38	-0.34	-0.52	-2.03	-1.13				
1.002	0.850	0.613						
0.983	0.845	0.610						
-1.86	-0.54	-0.51						

(*) Reference

Shin-Kori Unit-1 Cycle-01 (EOC, HFP, ARO)								
0.849	0.884	0.952	1.199	0.969	0.954	1.139	0.867	
0.837	0.875	0.949	1.189	0.972	0.959	1.143	0.864	
-1.41	-1.05	-0.31	-0.80	0.31	0.51	0.31	-0.35	
0.884	0.919	1.237	0.985	1.248	0.968	1.178	0.781	
0.875	0.912	1.223	0.988	1.240	0.976	1.182	0.784	
-1.05	-0.71	-1.17	0.30	-0.64	0.82	0.30	0.41	
0.952	1.237	0.984	1.201	0.980	1.163	1.090	0.616	
0.949	1.223	0.986	1.195	0.986	1.164	1.093	0.616	
-0.31	-1.17	0.16	-0.53	0.65	0.11	0.26	0.01	
1.199	0.985	1.201	0.985	1.182	0.917	0.909		
1.189	0.988	1.195	0.992	1.184	0.927	0.903		
-0.80	0.30	-0.53	0.72	0.13	1.10	-0.65		
0.969	1.248	0.980	1.182	1.181	1.064	0.609		
0.972	1.240	0.986	1.184	1.186	1.067	0.607		
0.31	-0.64	0.65	0.13	0.45	0.27	-0.28		
0.954	0.968	1.163	0.917	1.064	0.751			RMS 0.61
0.959	0.976	1.164	0.927	1.067	0.745			Min 0.01
0.51	0.82	0.11	1.10	0.27	-0.80			Max 1.41
1.139	1.178	1.090	0.909	0.609				
1.143	1.182	1.093	0.903	0.607				
0.31	0.30	0.26	-0.65	-0.28				
0.867	0.781	0.616						
0.864	0.784	0.616						
-0.35	0.41	0.01						

(*) Reference

REFERENCES

- [1] K. Smith, et. al., SIMULATE-3 Methodology, Studsvik/SOA-92-02, (1992).
- [2] T. Downar, Y. Xu, V. Seker, "PARCS v3.0, Theory Manual", 2010.
PARCS Website: <https://engineering.purdue.edu/PARCS>
- [3] C. H. Lee, B. O. Jo, J. S. Song, H. Y. Kim, S. G. Ji, H. G. Joo, "Verification of Extended Nuclide Chain of MASTER with CASMO-3 and HELIOS", KAERI/TR-947/98
- [4] Eunki Lee, Yongbae Kim, Deokjung Lee, "An Performance test of Core-Reflector Boundary Conditions on Transient Non-Linear Coarse Mesh Finite Different Method Based on the NEM", KNS Fall, 1999.
- [5] Hyun Chul Lee, "Unified Nodal Method for Static and Transient Analysis of Power Reactor", Thesis for Ph. D., Seoul National University (August 2001).
- [6] Maria Pusa, "Rational approximations to the matrix exponential in burnup calculations", Nuclear Science and Engineering, PUBLICATION II, 169, 2, p. 155-167, 2011.
- [7] M. Ryu, et. al., "Preliminary Assessment of nTRACER and McCARD Direct Whole Core Transport Solutions to VERA Core Physics Benchmark Problems," Transactions-American Nuclear Society, Vol. 111, p. 1244-1247, 2014.
- [8] CASMO-4E: Extended Capability CASMO-4 User's Manual, SSP-09/442-U, Studsvik Sacondpower, 2009.
- [9] Sooyoung Choi, Hyunsuk Lee, Ser Gi Hong, and Deokjung Lee, "Resonance Self-Shielding Methodology of New Neutron Transport Code STREAM", J. Nucl. Sci. Technol., 52(9):1133-1150, 2015.

Fig. 5. BOC (top) and EOC (bottom) radial normalized power distribution for Shin-Kori Unit-1 cycle-01 [SIMULATE-3 vs. RAST-K 2.0]

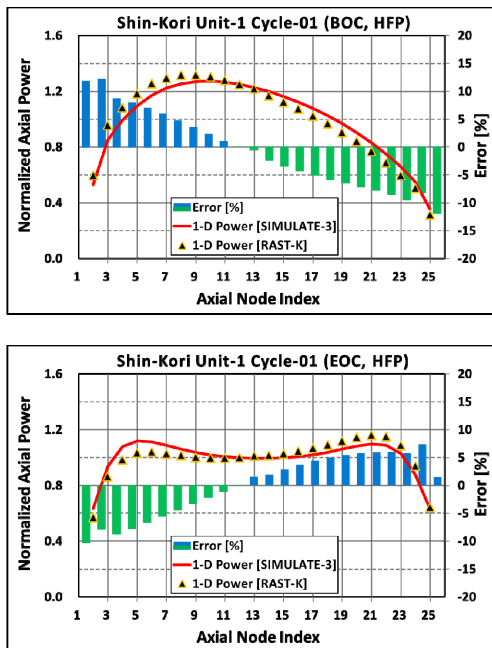


Fig. 6. BOC(top) and EOC(bottom) axial normalized power distribution for Shin-Kori Unit-1 cycle-01 [SIMULATE-3 vs. RAST-K 2.0]